

Mesoscopic photovoltaic effect in microjunctions

V. I. Fal'ko and D. E. Khmel'nitskiĭ

Institute of Solid State Physics, USSR Academy of Sciences

(Submitted 14 July 1988)

Zh. Eksp. Teor. Fiz. **95**, 328–337 (January 1989)

A mesoscopic photovoltaic (PV) effect in microjunctions is predicted. It comprises flow of direct current induced by applying a high-frequency magnetic field to the junction, and is due to the absence of an inversion center in a disordered sample of finite size. Regimes are considered with different irradiation intensities, frequencies, and temperatures. The characteristic scale of the PV current for an rf field of frequency 10^{10} Hz is of the order of 10^{-9} A. The PV current is a random function of the frequency and of the external magnetic field. The correlation functions of the currents at different values of these parameters are investigated.

Irradiation by an alternating field can cause direct current to flow in a medium without an inversion center. This phenomenon is called the photovoltaic (PV) effect.¹ Random distribution of impurities and defects in conductors may imitate local symmetry breaking. Nonetheless, at finite temperatures the PV currents from different parts of macroscopic samples cancel one another and the degree of asymmetry is negligibly small. This self-averaging takes place over scales larger than the length L_{in} on which inelastic processes or loss of phase coherence become significant for electrons of all existing energies. Over a scale $L \ll L_{in}$, the electron is scattered by a random potential coherently,² so that a conductor of size smaller than the inelastic length has no inversion center and finite PV current can flow in it. We consider here microscopic junctions of just this type (called mesoscopic). At temperatures of order 1 K their dimensions are on the order of microns.

In Sec. 1 we propose a very simple estimate of the PV effect in a mesoscopic sample and calculate the rms value of the PG tensor for high-frequency ($\omega\tau_f \gg 1$) fields.¹⁾ In Sec. 2 are investigated mesoscopic PV regimes in fields of varying intensity and frequency and at various temperatures. Section 3 is devoted to the correlation properties (relative to the applied magnetic field and the frequency) of PV currents in mesoscopic samples.

We define the microjunction as a metallic bridge of conductance G ($G\hbar/e^2 \gg 1$) joining bulky samples. The smallness ($L \ll L_{in}$, L_T) of the junction is bounded here by the mean free path, $L \gg l$, so that a diffusion regime can set in. In other words, the mean free path l and time τ are the smallest quantities in the problem. The diffusion approximation restricts also the parameters of the irradiating field. We assume throughout that $\omega\tau \ll 1$ and $Eel/\hbar\omega \ll 1$.

1. PV EFFECT IN A HIGH-FREQUENCY FIELD

Photovoltaic current is made to flow through a junction by the electron redistribution caused by an alternating field. In a unit time, each of $N \sim \sigma E^2 V/\hbar\omega$ electrons in a volume V absorbs a photon of energy $\hbar\omega$. These nonequilibrium electrons can diffuse in a time $\sim \tau_f$ to the banks of the junction. Since the junction has no inversion center, different numbers of electrons go off to its left and right banks. The degree of junction asymmetry can be estimated at the ratio of the characteristic mesoscopic fluctuation e^2/\hbar (Ref. 2) of its conductance to the conductance $G = \sigma V/L^2$ itself:

$$\alpha \sim \frac{e^2}{\hbar G} = \frac{e^2}{\hbar} \frac{L^2}{\sigma V}. \quad (1.1)$$

The degree of asymmetry $\alpha(\varepsilon)$ is a random function of the electron excitation energy, and the scale of its variation is $\delta\varepsilon \sim \hbar\tau_f^{-1}$. The contributions to the PV current from the electrons from different correlated energy intervals (of width $\sim \hbar\tau_f^{-1}$) have therefore random signs. Since the non-equilibrium carriers are distributed in a limited range $\hbar\omega$ near the Fermi energy, the number of such independent intervals is $n \sim \omega\tau_f$. After mutual cancellation of the random-sign currents from different intervals, the remaining effective contribution to the fluctuating current comes from $(\omega\tau_f)^{-1/2}$ electrons, and the PV current can be estimated at

$$I_{\Phi} \sim e \frac{N}{n^{1/2}} \alpha = e \left(\frac{\omega}{\tau_f} \right)^{1/2} \left(\frac{EeL}{\hbar\omega} \right)^2. \quad (1.2)$$

We have applied the foregoing reasoning only to high-frequency fields with $\omega\tau_f = n \gg 1$. We have also disregarded in the estimate (1.2) the dynamic action of the field on the electron diffusion via relaxation of its energy and phase. This can be done if, during the time τ_f of diffusion through the junction, the electrons contributing to the photocurrent absorb (emit) an $\hbar\omega$ photon not more than once. The total number of photons absorbed per unit time is $N \sim \sigma E^2 V/\hbar\omega$, and the number of such interactions per asymmetric electron during the time of flight is $\sim (EeL/\hbar\omega)^2$. Equation (1.2) pertains therefore to fields with $EeL/\hbar\omega \ll 1$.

The PV effect in weak fields can be described phenomenologically as follows. We expand the current in a homogeneous medium in powers of \mathbf{E}_ω . Contributing to the dc component of the current are terms of even power in the field, and in the leading order we have

$$I_{\Phi}^h = \beta_{lm}^h E_l^* E_m = S_{lm}^h E_l^* E_m + iA_l^h [EE^*]_l. \quad (1.3)$$

The real and imaginary parts of the PV tensor describe photocurrents called linear and circular, respectively. Under time reversal, the current reverses sign and \mathbf{E} goes over into \mathbf{E}^* . The symmetric tensor S therefore reverses sign for $t \rightarrow -t$, and the antisymmetric tensor A is transformed into itself. This means that the linear PV effect must be due to absorption of the irradiating field, while the circular one is possible also in the absence of dissipation.

The PV tensor in a microjunction, averaged over the different realizations of a random potential, is $\beta = 0$ and we

shall be interested hereafter in its mean square value $\overline{\beta\beta}$. To calculate this quantity it is convenient to use a Keldysh diagram technique, with matrix-type Green's functions

$$G = \begin{bmatrix} G^a & G^K \\ 0 & G^r \end{bmatrix}. \quad (1.4)$$

At equilibrium, the Keldysh function is

$$G^K = (1 - 2n(\epsilon)) (G_e^r - G_e^a). \quad (1.4')$$

The current in terms of the Keldysh function is given by

$$I(t) = \frac{e\hbar}{2m} \lim_{\eta \rightarrow 0} \int dS (\nabla - \nabla') G^K \left(\mathbf{x}, t + \frac{\eta}{2}; \mathbf{x}', t - \frac{\eta}{2} \right) \\ = \frac{e\hbar}{2m} \int d\epsilon dS [(\nabla - \nabla') G_e^K(\mathbf{x}, \mathbf{x}')]_{\mathbf{x}=\mathbf{x}'}. \quad (1.5)$$

Expanding in (1.5) G^K in a perturbation theory in terms of the external field, we verify that graphically the PV tensor is described by triangular diagrams such as in Fig. 1. In the diffusion approximation the rms FG tensor is determined by the sum of different diagrams of type a-c in Fig. 2. The ladders in these diagrams correspond to two-particle Green's functions (cooperon and diffusion)

$$P_{e-e'}(\mathbf{x}, \mathbf{x}') = \overline{G_e^r(\mathbf{x}, \mathbf{x}') G_e^a(\mathbf{x}, \mathbf{x}')}, \quad (1.6)$$

which satisfy in the absence of external fields the equation

$$(i\Omega - D\nabla^2) P_a(\mathbf{x}, \mathbf{x}') = 2\pi\nu\delta(\mathbf{x} - \mathbf{x}') \quad (1.7)$$

with boundary conditions $P\Omega = 0$ on the banks and $\mathbf{n}\cdot\nabla P = 0$ on the walls of the junction.

If $\omega\tau_f = \omega L^2/D \gg 1$, terms of the form $P_\Omega^2 P_{\Omega+2\omega}$ and so on are small, and the main contribution to the correlator $\beta\beta$ are made by products of diffusions of type P_Ω^3 , which correspond to diagrams of type a in Fig. 2. As a result, the squared PV current averaged over different realizations of the random potential is given by

$$\overline{I_{ph}^2} = \frac{2D^3}{(\pi\nu)^4} \left(\frac{Ee}{\hbar\omega} \right)^4 \sum_q \int d\Omega |P_a(\mathbf{q})|^4 (D\mathbf{q}^2 + \tau_{in}^{-1}) \\ \times [n(\epsilon) - n(\epsilon - \omega)] [n(\epsilon + \Omega) - n(\epsilon + \Omega - \omega)], \quad (1.8)$$

and depends only on the ac-field power. The circular part of the mesoscopic PV current is thus negligibly small. This means that in the regime considered the irradiating-field dissipation is substantial, and the calculation accords fully with the proposed qualitative description. The linear PV current is determined by the symmetric tensor $\beta_{lm}^x = s_{lm}^x$ with the value

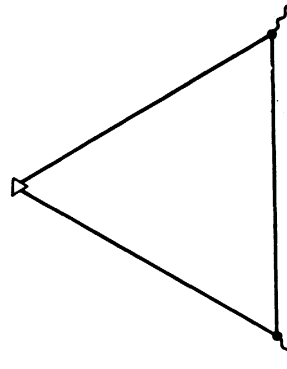


FIG. 1. Feynman diagrams for PV current.

$$\overline{\beta^2} = 4 \frac{e^2\omega}{\tau_f} \left(\frac{eL_x}{\hbar\omega} \right)^4 \frac{V_d}{L_x^d} \begin{cases} 8\pi/45, & L_x \gg L_{y,z} \\ 4\zeta(3)/\pi^2, & L_{x,y} \gg L_z \\ 3/8, & L_{y,z} \gg L_x \end{cases} \quad (1.9)$$

which is calculated from (1.8) and refines the estimate (1.2) to satisfy junctions with different effective dimensionalities.

2. PV REGIMES IN A MICROJUNCTION

We analyze in this section the mesoscopic PV effect, without the constraint that $(\omega\tau_f)^{-1}$ and $EeL/\hbar\omega$ be small. This can be done if one knows the correlation function of the currents at different instants of time Θ_1 and Θ_2 :

$$K(\Theta_1, \Theta_2) = \overline{I(\Theta_1)I(\Theta_2)}. \quad (2.1)$$

The squared photocurrent averaged over different realizations of the random potential is the part of (2.1) which does not depend on the times Θ_1 and Θ_2 :

$$\overline{I_{ph}^2} = \lim_{\theta \rightarrow \infty} \theta^{-2} \iint_0^\theta d\Theta_1 d\Theta_2 K(\Theta_1, \Theta_2), \quad (2.2)$$

Expressions for the correlator (2.1) can be obtained by generalizing the equations of Ref. 3 to include alternating fields:

$$K(\Theta_1, \Theta_2) = \frac{4}{(2\pi\nu)^4} \left(\frac{eD}{L_x} \right)^2 \int \dots \int d\mathbf{x}_1 d\mathbf{x}_2 d\Theta_2' d\Theta_2' \\ \times \lim_{x_i' \rightarrow x_i} \left\{ P_{\gamma}^d(\gamma_1, \mathbf{x}_1; \Theta_1' - \frac{\gamma}{2}, \mathbf{x}_2) \right. \\ \times P_{[-\gamma]}^d \left(\frac{\gamma_1}{2}, \mathbf{x}_1; \Theta_2' + \frac{\gamma}{2}, \mathbf{x}_2 \right) \\ \left. \times \nabla_{\mathbf{x}_1}^k \nabla_{\mathbf{x}_1'}^k F_1 + P_{[2\gamma]}^c \left(\frac{\rho_1}{2}, \mathbf{x}_1; \gamma_1' - \Theta_2, \mathbf{x}_2 \right) \right\}$$

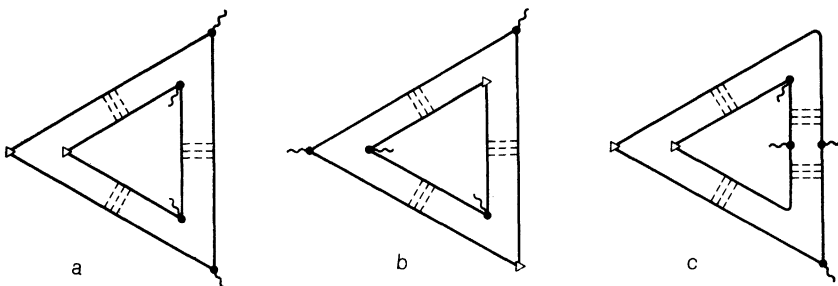


FIG. 2. Diagrams for rms value of PV current in the diffusion approximation, obtained by perturbation theory.

$$\begin{aligned}
& \times P_{[2\gamma_1]}^c \left(\frac{\rho_2}{2}, \mathbf{x}_2; \gamma_2', -\Theta_1, \mathbf{x}_1 \right) \nabla_{\mathbf{x}_1}^k \nabla_{\mathbf{x}_2}^k F_2 \\
& + 2 \left[\nabla_{\mathbf{x}_2}^d P_{\rho_1}^d \left(\gamma_1', \mathbf{x}_1; \Theta_2' - \frac{\rho_1}{2}, \mathbf{x}_2 \right) \right] \\
& \times \left[\nabla_{\mathbf{x}_1}^d P_{[-\rho_2]}^d \left(\gamma_2', \mathbf{x}_2; \Theta_1 - \frac{\rho_2}{2}, \mathbf{x}_1 \right) \right] F_3 \\
& + 2 P_{[2\gamma_2]}^c \left(\frac{\rho_2}{2}, \mathbf{x}_2; \gamma_2' - \Theta_1, \mathbf{x}_1 \right) \\
& \times \left(\nabla_{\mathbf{x}_1}^c \nabla_{\mathbf{x}_2}^c P_{[2t_1]}^c \left(\frac{\xi_2}{2}, \mathbf{x}_1; \frac{\xi_1}{2}, \mathbf{x}_2 \right) \right) F_4 \}, \quad (2.3)
\end{aligned}$$

where

$$\nabla^{(k, d, c)} = \partial - i \frac{e}{c} \mathbf{A}^{(k, d, c)},$$

$$F_1 = \overline{G_{\xi_1}^K}(\mathbf{x}_2', t_1) \overline{G_{[-\xi_1]}^K}(\mathbf{x}_2, t_1'), \quad F_i = \overline{G_{\xi_i}^K}(\mathbf{x}_1, t_i) \cdot \overline{G_{[-\xi_i]}^K}(\mathbf{x}_2, t_i'),$$

$$\gamma = \Theta_1 - \Theta_2, \quad \gamma_1 = (\Theta_1 + \Theta_2)/2, \quad \gamma_1' = (\Theta_1' + \Theta_2)/2,$$

$$\rho_i = \Theta_1 - \Theta_i', \quad \xi_{1,3} = \pm \rho_2 - \rho_1, \quad \xi_i = \rho_i, \quad \xi_2 = 2(\gamma_1' - \gamma_2'),$$

$$t_{1,2,3} = (\Theta_1' + \Theta_2' - \gamma)/2, \quad t_4 = \gamma_1',$$

$$t_{1',2,3} = (\Theta_1' + \Theta_2' + \gamma)/2, \quad t_4' = \Theta_2 - \rho_1/2.$$

Each term in (2.3) corresponds to one of the diagrams of Fig. 3. The two-particle Green's functions $P_{\eta}^{c(d)}(t, \mathbf{x}; t', \mathbf{x}')$ (cooperon and diffusion) satisfy the equation⁴

$$\begin{aligned}
& \left\{ \partial_t - D \left(\partial - i \frac{e}{c} \mathbf{A}^{(c, d)} \right)^2 - ie\varphi^{(c, d)} + \tau_{in}^{-1} \right\} P_{\eta}(t, \mathbf{x}; t', \mathbf{x}') \\
& = 2\pi\nu\delta(t - t')\delta(\mathbf{x} - \mathbf{x}') \quad (2.4)
\end{aligned}$$

with boundary conditions $P=0$ on the banks and $\mathbf{n}(\partial - ie\mathbf{A}^{(c, d)}/c)P=0$ on the walls of the junction. In a gauge with a zero vector potential it is necessary to use in Eq.(2.4) $\varphi^d = 2xE \sin(\omega\eta/2) \sin\omega t$ for the diffusion and

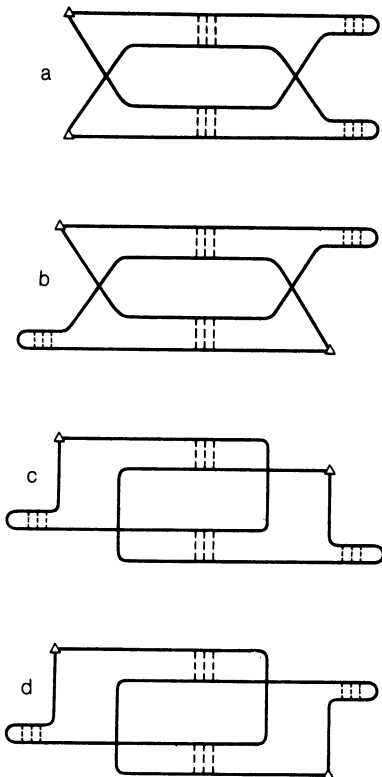


FIG. 3. Current-correlator diagrams in the diffusion approximation.

$\varphi^c = xE \sin(\omega t/2) \sin\omega\eta$ for the cooperon.

The Keldysh functions $\overline{G^K}$ averaged over the impurity positions correspond to the subs on the diagrams of Fig. 3. In the same gauge we have

$$\{\partial_t - D\partial^2 - 2ieEx \sin(\omega\eta/2) \sin\omega t\} \overline{G_{\eta}^K}(t, x) = 0 \quad (2.5)$$

and on the junction banks

$$\begin{aligned}
& \overline{G_{\eta}^K} \left(x = \pm \frac{L}{2} \right) \\
& = \overline{G_{eq}^K}(\eta) \exp \left\{ \pm i \frac{LeE}{\hbar\omega} \sin \frac{\omega\eta}{2} \cos\omega t \right\}. \quad (2.5')
\end{aligned}$$

The time representation for the equilibrium Keldysh function $\overline{G_{eg}^K}$ is obtained from (1.4') by a Fourier transformation, and it is convenient to separate this function in $\overline{G^K}$ as a factor independent of t and x :

$$\overline{G_{\eta}^K}(t, x) = 4\pi\nu \frac{\pi T}{\text{sh}(\pi T\eta)} \Psi_{\eta}(\mathbf{x}, t) \approx \frac{4\pi\nu}{\eta} \Psi_{\eta}(\mathbf{x}, t) \text{ as } T \rightarrow 0. \quad (2.6)$$

Now that we have described completely all the elements of the correlator (2.3), we can track the various asymptotic regimes of the mesoscopic FV effect. For simplicity, we confine ourselves to the time being to the limit $T=0$, in which no account is taken of the smearing of the Fermi distribution function and of the inelastic relaxation. It follows from (2.4) and (2.5) that the times during which the functions P and $\overline{G^K}$ vary are determined either by the frequency of the external field or by the characteristic value Λ_0 of the diffusion operator:

$$\Lambda = -D\partial^2 - ix e E(t, \eta)/\hbar. \quad (2.7)$$

The relation between these two quantities demarcates the boundary between the regions of the high-frequency and quasistationary fields. On the other hand, the operator (2.7) depends on the ratio of the contact dimensions to the length $L_E \sim (\hbar D/eE)^{1/3}$ starting with which the field begins to influence substantially the character of the diffusion ($D\nabla^2 \sim eEx/\hbar$). If $L_E \gg L$, we have $\Lambda_0 \sim \pi^2\tau_f^{-1}$, but for the inverse inequality we have $\Lambda_0 \sim (DE^2e^2/\hbar^2)^{1/3}$. In the former case ($EeL^3/\pi^2\hbar D \ll 1$) we can regard as low a frequency $\omega \ll \Lambda_0 = \pi^2\tau_f^{-1}$. In the latter case a high-frequency field has $\omega \ll \Lambda_0 = (DE^2e^2/\hbar^2)^{1/3}$.

Figure 4 shows the characteristic asymptotic regions of this problem. The coordinates are the dimensionless frequencies $\omega = \omega\tau_f\pi^{-2}$ and the amplitude $\varepsilon = LLe\tau_f/\hbar\pi^2$ of the external field. A weak low-frequency field corresponds to the region 1, in which the time dependences in Eqs. (2.5) and (2.5') need be accounted for only in the boundary conditions. Expressions for the cooperon and diffusion in this region can be obtained by perturbation theory in terms of the field. The rms PV current calculated in this manner is of the form

$$\overline{I_{ph}^2} = 4 \left(\frac{e}{\tau_f} \right)^2 \left[\frac{LLe\tau_f}{\pi^2\hbar} \right]^4 \frac{V_d}{L_x^d} \begin{cases} 0.335, & L_{y,z} \ll L_x \\ 0.317, & L_z \ll L_x \ll L_y \\ 0.209, & L_x \ll L_{y,z} \end{cases} \quad (2.8)$$

This result agrees with the description obtained in Ref. 3 for

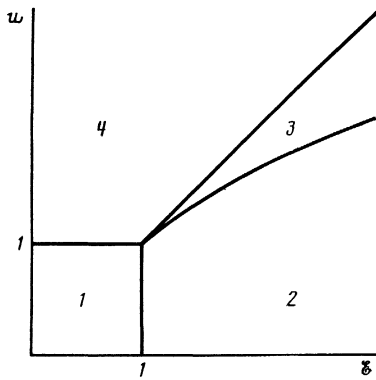


FIG. 4. Typical asymptotic regions for the irradiating-field parameters. The symbols $\omega = \omega\tau_f\pi^{-2}$ and $\varepsilon = LE\tau_f/\hbar\pi^2$ denote the field frequency and amplitude nondimensionalized by the time of flight.

the mesoscopic fluctuations of the current-voltage characteristic. The current-fluctuations correlator $\overline{\delta I(V)\delta I(V')}$ in a one-dimensional junction, calculated in Ref. 3, can be made more accurate in the ohmic regime to include terms of higher order in the drawing fields V and V' :

$$\overline{\delta I(V)\delta I(V')}$$

$$\overline{I_{ph}^2} = \frac{e^2\omega}{\tau_f} \begin{cases} 20 \left[\ln^2 \left(\frac{eEL_x}{\hbar\omega} \right) - 3.88 \ln \left(\frac{eEL_x}{\hbar\omega} \right) + 1.46 \right], & L_x \gg L_{E,y,z} \\ \sim \left(\frac{L_y E e}{\hbar\omega} \right) \ln^2 \left(\frac{eEL_x}{\hbar\omega} \right), & L_x \ll L_E \ll L_{E,y} \\ \sim \left(\frac{L_y E e}{\hbar\omega} \right) \left(\frac{L_z E e}{\hbar\omega} \right) \ln^2 \left(\frac{eEL_x}{\hbar\omega} \right), & L_E \ll L_{E,y,z} \end{cases} \quad (2.10)$$

The asymptotic behavior of the PV current in region 2 can be obtained by matching the results on the region boundaries. For a transition regime to exist between the weak (2.8) and strong low-frequency fields, the mean square PV current should be in the considered region a function $F(\varepsilon)$ of only one parameter ε . The specific form of this function is determined from the requirement that $F(\varepsilon)$ and (2.10) be equal on the line $\omega^3/\varepsilon^2 = 1$. For $\varepsilon \gg (\omega^3/1)$ we have therefore

$$\overline{I_{ph}^2} \sim \left(\frac{e}{\tau_f} \right)^2 \mathcal{E}^{d+1/2} \ln^2 \mathcal{E} \frac{V_d}{L_d^d}. \quad (2.11)$$

Equations (2.8)–(2.11) give the most optimistic estimate of the considered effect. A finite temperature suppresses the photocurrent both via relaxation processes and via smearing of the equilibrium distribution function. Energy and phase relaxation cause the electron scattering to be coherent only in regions for which $L \ll L_{in}$. Each of these regions make an independent contribution to the photocurrent, resulting in strong self-averaging. The temperature smearing of the equilibrium distribution function brings into play supplementary correlated energy interval, and this leads likewise to self-averaging of the PV current. Thus, in region 3 the current through a one-dimensional conductor

$$\approx \left(\frac{e}{\tau_f} \right)^2 \left[\frac{(V+V')e\tau_f}{\pi^2\hbar} \right]^2 \left\{ 1 + a \left[\frac{(V-V')e\tau_f}{\pi^2\hbar} \right]^2 + \dots \right\}. \quad (2.9)$$

The first term of this expansion describes the junction-conductance fluctuations.⁵ The next term of the expansion in the fields is due to the differences between the currents $|I(\pm V)|$ flowing in the junction at different signs of the applied voltage. The PV current is determined in the quasi-stationary limit by just this term, and by replacing in the second term of (2.9) the quantity $V \pm V'$ by the amplitude LE of the alternating field we obtain an estimate that agrees with (2.8) apart from a numerical factor.

The high frequencies $\omega\tau_f\pi^{-2} \gg 1$ and $\hbar^2\omega^3/DE^2e^2 \gg 1$, at which the field changes many times during the time of flight through the junction (or during the time of the electron phase and energy relaxation) correspond to regions 3 and 4 of Fig. 4. Of help in separation of these regions are the boundary conditions (2.5') on the Keldysh function, which contain the parameter $LEe/\hbar\omega$. Weak fields correspond to region 4, in which Eq. (1.9) obtained by perturbation theory is valid. Region (3), where $\varepsilon \gg \omega \gg \varepsilon^{2/3}$, pertains to strong high-frequency fields in which the diffusion is far from free. Strong fields not only produce the nonequilibrium carriers that contribute to the PV current, but lead also to energy relaxation of the same carriers. As a result, the quadratic current growth (1.9) (as a function of field) is replaced in region 3 by the weaker dependences

($L_{y,z} \ll L_{E,x}$) senses the temperature starting with which $\min\{\tau_{in}, \tau_t = \hbar/\pi T\} \gtrsim \omega^{-1}$:

$$\overline{I_{ph}^2} \approx 20 \frac{e^2\omega}{\tau_f} \ln^2 \left(\frac{LeE\tau_{(t,n,T)}}{\hbar} \right). \quad (2.12)$$

Further increase of the temperature $\tau_{(T,in)} \sim \hbar/LeE$ eliminates the difference between the strong and weak fields (in the classification of Fig. 4). Calculations of the PV effect at sufficiently high temperatures are therefore possible by perturbation theory, as in the derivation of Eqs. (1.9) and (2.8). The results of these calculations at different ratios of the problem parameters can be conveniently written in the form

$$\overline{I_{ph}^2} = \frac{1}{4} \lambda \left(\frac{e}{\tau_0} \right)^2 \left(\frac{L_0 e E}{\hbar\Omega_0} \right)^4 \frac{V_d}{L_0^d} u(\omega) t \quad (2.13)$$

where

$$L_0 = \min\{L_x, L_{in}\}, \tau_0 = L_0^2/D, \Omega_0 = \max\{\pi^2\tau_f^{-1}u(\omega), \tau_{in}^{-1}\}, \\ u(\omega) = \max\{1, \pi^{-2}\omega\tau_f\}, t = \min\{1, \hbar u(\omega)\pi^2/T\tau_f\}, \quad (2.14)$$

V_d is the volume of a junction with effective dimensionality d . The values of the numerical factor λ for different asymp-

TABLE I. Values of the coefficient λ [see (2.13)].

L_0	$u(\omega)$	Ω_0	t	$d=1$	$d=2$	$d=3$
L_x	$\omega\tau_f\pi^{-2}$	ω	1	$8\pi^3/45$	$4\zeta(3)$	$2\pi^2/3$
L_{in}	$\omega\tau_f\pi^{-2}$	ω	1	$4\pi^3$	$4\pi^2$	$4\pi^2$
L_x	$\omega\tau_f\pi^{-2}$	ω	ω/T	$4\pi^3/135$	$4\zeta(3)/3$	$\pi^2/9$
L_{in}	$\omega\tau_f\pi^{-2}$	ω	ω/T	$4\pi^3/3$	$2\pi^2/3$	$\pi/12$
L_x	1	$\pi^2\tau_f^{-1}$	1	0,335	0,317	0,209
L_{in}	1	τ_{in}^{-1}	1	$5\pi/16$	$1/8$	$1/82$
L_x	1	$\pi^2\tau_f^{-1}$	$\hbar\pi^2/T\tau_f$	$0,42\pi^2$	$0,26\pi^2$	$0,5\pi^2$
L_{in}	1	τ_{in}^{-1}	$\hbar\pi^2/T\tau_f$	$\pi^2/768$	$\pi/1152$	$\pi/1536$

Note. When using the table, the values of L_0 , $u(\omega)$, Ω_0 , and t must be determined from Eqs. (2, 14), and the row corresponding to these values in the table must then be found. The values of the coefficient λ for different d ($d=1,2,3$) are given in the three right-hand columns of this row. For example, the first row of the table corresponds to Eq. (1.9) in Sec. 1.

otic cases, as functions of the parameters (2.4), are listed in Table I.

It is seen from (2.13) and (2.14) that the optimal conditions under which the mesoscopic PV effect can be investigated are determined by the relations $\omega \sim \tau_f^{-1}\pi^2 \sim \tau_{in}^{-1}$. At the values $\tau_{in} \sim 10^{-10}$ s typical of metals the PV current is of the order of $I_{ph} \sim 10^{-9}$ A.

3. CORRELATION PROPERTIES OF MESOSCOPIC PV CURRENTS

Just as the conductance of a mesoscopic sample,⁵ the PV current through it is sensitive to the applied magnetic field. It is convenient to describe the influence of the magnetic field by the correlation function

$$K(H, \Delta H) = \overline{I_{ph}(H + \Delta H/2)I_{ph}(H - \Delta H/2)}. \quad (3.1)$$

At $H = \Delta H = 0$ the function $K(0,0)$ coincides with the already calculated rms PV current. To analyze this function for $H, \Delta H \neq 0$ it is necessary to take into account in (2.4) the nonzero vector potential.

The value of the magnetic field H is connected with A^c in the equation for the cooperon by the relation $\text{curl } A^c = 2H$. Therefore allowance for the magnetic field leads to suppression of the contribution of the cooperon diagrams of form b and d in Fig. 3, meaning also to a decrease of the effect in these regions on Fig. 4, where these diagrams play an important role. These are the high-frequency regions with $\omega \gg \Omega_0$. When the field increases to $H_c \sim \Phi_0/L_x L$ ($\Phi_0 = 2\pi\hbar c/e$ is the flux quantum), the amplitude of the effect is systematically suppressed. In fields stronger than H_c the contributions of the diagrams with the cooperons are already completely suppressed and no further change of the PV current amplitude should take place all the way to fields $\omega_c \tau \sim 1$.

The vector potential A^d in (2.4) is connected with the field ΔH by the relation $\text{curl } A^d = \Delta H$. As a result, the correlator (3.1) attenuates over a scale $\Omega H_c \sim \Phi_0/L_x L_1$, i.e., when the magnetic field is changed the PV current undergoes irregular random changes with correlations (relative to the magnetic field) within the scale of ΔH_c . In low-frequency fields, the amplitude of such oscillations is almost insensitive to the magnetic field, which in high-frequency fields it is subject to the suppression described above.

In three-dimensional systems, the magnetic-field scales over which the correlator (3.1) changes correspond to the

magnetic-field flux of order Φ_0 regardless of the field direction. This is not the case in two-dimensional systems. A magnetic field perpendicular to a two-dimensional layer leads to dephasing of the electrons, and is characterized by a scale Φ_0/L^2 . The mechanism of the effect parallel to the layer is connected with the Zeeman splitting $\Delta\varepsilon = 2\mu gH$ of the magnetic-field spin states. The degree α of asymmetry of the junction differs greatly for different spin states of $\Delta\varepsilon\tau_f = 2\mu gH\tau_f > 1$. The characteristic scale of the parallel magnetic field in which oscillations of the PV current take place in two-dimensional structure is therefore

$$H_c' \sim (\hbar/\mu g) \max\{\pi^2\tau_f^{-1}, \omega\} \sim H_c^{\perp} (D\hbar m/g) \max\{1, \omega\tau_f\pi^{-2}\} \sim H_c^{\perp} \cdot 10^2 \max\{1, \omega\tau_f\pi^{-2}\}.$$

A chemical-potential change larger than $\Delta\mu_c \sim \hbar\tau_f^{-1}$ (Ref. 6) also upsets the correlation of the PV currents. Such an effect can be obtained in point contacts of silicon field-effect-transistor inversion layer by varying the gate voltage.

Another characteristic mesoscopic feature of the effect are the frequency correlation properties of the PV current. They can be conveniently described by the correlation function of PV currents having different frequencies:

$$K(\omega, \Delta\omega) = \overline{I_{ph}(\omega + \Delta\omega/2)I_{ph}(\omega - \Delta\omega/2)}. \quad (3.2)$$

As seen from (1.9) and (2.8)–(2.11), a frequency dependence of the effect has meaning only at frequencies $\omega\tau_f \gg 1$. So long as $\Delta\omega \ll \omega$, the main contribution to (2.3), just as in Sec. 1, comes from diagrams of type a in Fig. 2. Now, however, these diagrams correspond to cooperon and diffusion products of the form $P_{\Omega}^2 P_{\Omega \pm \Delta\omega}$ which leads to

$$K(\omega, \Delta\omega) = \frac{2D^3}{(\pi v)^4} \left(\frac{Ee}{\hbar\omega} \right)^4 \sum_q \int d\Omega |P_{\Omega}|^2 |P_{\Omega+\Delta\omega}|^2 \chi(Dq^2 + \tau_{in}^{-1}) [n(\varepsilon) - n(\varepsilon - \omega - \Delta\omega/2)] \chi[n(\varepsilon + \Omega) - n(\varepsilon + \Omega - \omega + \Delta\omega/2)]. \quad (3.3)$$

Integration in (3.3) with disregard of τ_{in}^{-1} and of the smearing of the Fermi step yields

$$K(\omega, \Delta\omega) = \frac{e^2\omega}{\tau_f} \left(\frac{eEL_{\Delta\omega}}{\hbar\omega} \right)^4 \begin{cases} 16\pi \left[R \frac{\text{sh } R + \sin R}{\text{ch } R - \cos R} - 2 \right], & d=1 \\ \frac{V_d}{L_{\Delta\omega}^d} \text{ for } \Delta\omega \gg \tau_f^{-1}\pi^2, & d=2, 3 \end{cases}, \quad (3.4)$$

where $L_{\Delta\omega} = (D/\Delta\omega)^{1/2}$ and $R = L_x/L_{\Delta\omega}$. It is seen from (3.4) that the correlation of the PV currents is strongly suppressed already at a frequency difference $\Delta\omega_c \sim \tau_f^{-1}\pi^2$. The PV current in a high frequency field, outside the $\Delta\omega_c$ scale, is therefore a random function of the frequency. A particular manifestation of this fact is that when the field frequency is changed by $\Delta\omega > \Delta\omega_c$ a change takes place not only in the magnitude of the PV current but also in its direction.

The polarization properties of the effect can be investigated with the aid of the correlator $K(J_{ij}, J'_{ij})$ of the PV currents produced by monochromatic fields with different polarization tensors $J_{ij} = \langle E_i E_j^* \rangle$. In weak high-frequency fields this correlator can be calculated in the same way as the mean square PV current (1.8), and the result of this calculation is

$$K(J, J') = \overline{\beta^3} \text{Sp}(JJ'), \quad (3.5)$$

where $\overline{\beta^2}$ is defined by Eq. (1.9). It follows from (3.5), in particular, that there is no correlation between currents due to irradiation by fields with perpendicular linear polarization directions ($K(\mathbf{E}, \mathbf{E}') \sim |\mathbf{E}_\omega \mathbf{E}'_\omega|^2$).

Experimental investigations of the indicated correlation properties of the mesoscopic PV effect should be carried out in low-intensity fields, to prevent noticeable heating of

the sample. Otherwise annealing of the sample may occur and alter substantially the specific realization of the random potential in which all the described phenomena take place. This will upset the correlations of the PV currents.

In conclusion, the authors are grateful to S. V. Meshkov and V. V. Tatarskiĭ for advice on the numerical calculations.

¹⁾ $\tau_f = L^2/D$ is the time of the diffusive passage through the junction. The condition $L \ll L_{in}$ should be met for electrons with energies $|\varepsilon - \varepsilon_F| \lesssim \max\{\hbar\tau_f^{-1}, \hbar\omega\}$.

¹⁾ V. I. Binicher and B. I. Sturman, Usp. Fiz. Nauk **130**, 415 (1980) [Sov. Phys. Usp. **23**, 199 (1980)].

²⁾ B. L. Al'tshuler, Pis'ma Zh. Eksp. Teor. Fiz. **41**, 530 (1985) [JETP Lett. **41**, 648 (1985)]. P. A. Lee and D. A. Stone, Phys. Rev. Lett. **55**, 1622 (1985).

³⁾ A. I. Larkin and D. E. Khmel'nitskiĭ, Zh. Eksp. Teor. Fiz. **91**, 1815 (1985) [Sov. Phys. JETP **64**, 1075 (1985)].

⁴⁾ B. L. Altshuler, A. G. Aronov, and D. E. Khmel'nitskiy, J. Phys. C15, 7367 (1985).

⁵⁾ B. L. Al'tshuler and D. E. Khmel'nitskiĭ, Pis'ma Zh. Eksp. Teor. Fiz. **42**, 291 (1985) [JETP Lett. **42**, 359 (1985)]. P. A. Lee, D. A. Stone, and H. Fukuyama, Phys. Rev. B **35**, 1039 (1987).

⁶⁾ W. J. Skocpol, P. M. Mankievich, R. E. Howard, *et al.*, Phys. Rev. Lett. **56**, 2865 (1986).

Translated by J. G. Adashko